Short Communication

Quantum Chemical Studies on the Corrosion Inhibition of Fe₇₈B₁₃Si₉ glassy alloy in Na₂SO₄ Solution of Some Thiosemicarbazone Derivatives

Murat Saraçoğlu[1,], Mahmooud Ibrahim A. Elusta[2], Savaş Kaya[3], Cemal Kaya[3], Fatma Kandemirli[4]*

[1] Faculty of Education, Erciyes University, 38039 Kayseri, Turkey
[2] Department of Materials Science and Engineering, Kastamonu University, 37150, Kastamonu, Turkey
[3] Cumhuriyet University, Faculty of Science, Department of Chemistry, 58140, Sivas, Turkey
[4] Department of Biomedical Engineering, Faculty of Engineering and Architecture, Kastamonu University, 37150, Kastamonu, Turkey
*E-mail: muratsaracoglu@gmail.com

In this study, the density functional theory (DFT) at the gradient-corrected correlation functional of Lee-Yang-Parr (B3LYP) functional with 6-311++G(2d,2p), correlation-consistent, polarized valence, X-zeta (cc-pVTZ) basis sets, BP86 functional with/6-311++G(2d,2p) basis set and ab initio calculations using the Hartree-Fock (HF)/6-311++G(2d,2p) methods in gas and water phase of neutral and protonated forms of molecules were performed on six thiosemicarbazone derivatives, namely 4-methyl acetophenone thiosemicarbazone (Inh 1), 4-methoxy acetophenone thiosemicarbazone (Inh 2), Benzaldehyde thiosemicarbazone (Inh 3), 4-methoxy benzaldehyde thiosemicarbazone (Inh 4), 4-ethyl benzaldehyde thiosemicarbazone (Inh 5) and 4-bromo benzaldehyde thiosemicarbazone (Inh 6). The quantum chemical parameters/descriptors, namely, dipole moment (D), highest occupied molecular orbital energy (E_{HOMO}), lowest unoccupied molecular orbital energy (E_{LUMO}), HOMO-LUMO energy gap (ΔE), absolute electronegativity (χ), absolute hardness (η), softness (σ), proton affinity (PA), electrophilicity (ω) and nucleophilicity (ε) were calculated and correlated with the experimental inhibition efficiencies (%IE). It was observed that the theoretical and experimental results were in good agreement.

1. INTRODUCTION

Corrosion can be defined as the progressively destruction of especially metals by chemical reaction with various molecules in their environment [1]. The corrosion of metals commonly used in

industry leads to great economic loss. One of the most effective alternatives to protect the metals against this undesirable process is the use of the inhibitors that being adsorbed on metal surface. It is important to note that the most effective corrosion inhibitors are π-systems and heterocyclic organic compounds including heteroatoms such as O, N, S [2-4]. Corrosion inhibition process can be described as the formation of donor-acceptor surface complexes between vacant *d*-orbital of a metal with free or π-electrons of organic inhibitor, generally including aforementioned heteroatoms. The efficiency of a corrosion inhibitor against the corrosion of any metal depends on not only the characteristic of the environment and the structure of inhibitor but also the nature of metal surface. Experimental tools as weight loss, Electrochemical Impedance Spectroscopy, potentiodynamic polarization, Fourier transform infrared spectroscopy and Scanning Electron Microscopy are very useful to explain the inhibition mechanisms and inhibition efficiencies of corrosion inhibitors but it is known that these techniques are often expensive and time-consuming [5-8].

The anions such chloride, sulphate and bicarbonate as most commonly found in water causes corrosion and the effect on the corrosivity of the sulphate ions in water is greater than the chloride ion, however the bicarbonate ion demonstrates Inhibitive tendencies.

Sulfate coming from fuel during combustion in the gas turbine reacts with sodium chloride at high temperatures and sodium sulphate forms, then it deposits on the hot section Parts, such as rotary blades and nozzle guide vanes and, causing in accelerated oxidation attack [9].

Basim and et al. investigated corrosion rate of carbon steel in Sodium sulphate (Na_2SO_4) under flow conditions using rotating cylinder electrode (RCE) in range of 0-2000 rpm rotation velocity and 32-52 °C temperatures with electrochemical polarization technique (limiting current density) and weight loss method in different salt concentrations between 0.01 to 0.4 M. The results of Basim and et al. showed that the increase in rotational speed caused a significant increase in the corrosion rate represented by limiting the current density [10]. Sodium sulphite (Na_2SO_3) utilized as oxygen scavenger reacts with oxygen at low temperature and pressure and sodium sulphate occurs and causes severe attack to the tubes of the boiler [11].

Mrowczynski and Szklarska-Smialowska investigated inhibition effect of 6-10 carbon atoms normal aliphatic acids in the molecule in 0.05 M aerated solutions Na_2SO_4 in the pH range of 6-12 and they found that the depolarization of oxygen atom is not the only factor responsible from protection of the surface of iron metal in aerated solution containing a critical concentration of the inhibitor [12].

The performance of an organic inhibitor depends on the chemical structure and physicochemical properties of the molecules such as energy of frontier orbitals, electron density of donor atoms, hardness, softness, of the molecule. Quantum chemical calculations have been performed to study the mechanism of corrosion inhibition [13-28].

Many studies showed that thiosemicarbazone derivatives are quite effective corrosion inhibitors against the corrosion of various metals. Recently, Arab and Emran [29] studied the corrosion and corrosion inhibition of $Fe_{78}B_{13}Si_9$ glassy alloy with some thiosemicarbazone derivatives in 0.2 M Na_2SO_4 solution containing 10% MeOH and reported that the inhibition efficiency ranking for at 10^{-4} M acetophenone thiosemicarbazone compounds both electrochemical measurements are Inh 2>Inh 1 and for benzaldehyde thiosemicarbazone and its *p*-substituted derivatives is Inh 4>Inh 5>Inh 3>Inh 6.

Experimental results means are useful to explain the inhibition mechanism but they are often expensive and time-consuming. Developments in computer and software technology have led to the widespread use of theoretical chemistry in corrosion inhibition research. Several quantum chemical methods and molecular modelling techniques have been performed to correlate the inhibition efficiency of the inhibitors with molecular properties of inhibitors [30-39]. The reactive ability of the inhibitor is closely linked to their frontier molecular orbitals (MO) with highest occupied molecular orbital (HOMO) and lowest unoccupied molecular orbital (LUMO) and the other parameters such as hardness (η) and softness (σ). Recently, Density Functional Theory (DFT) has become an attractive theoretical method because it gives significant results for even big complex molecules at low cost [40-42].

In this study, a detailed quantum chemical studies of the Inh 1-6 molecules (**Figure 1**) have been performed using density functional theory (DFT) and ab initio methods within a standard Gaussian 09 (Revision B.05) [43]. The correlation between the quantum chemical parameters such as the frontier orbital energies, the energy gap between frontier orbital energies differences, hardness, softness, electrophilicity, nucleophilicity, proton affinity, dipole moment, Mulliken charges on heavy atoms and inhibition efficiency have been found and discussed in gas and water phase of neutral and protonated forms of molecules by using different methods and basis sets.
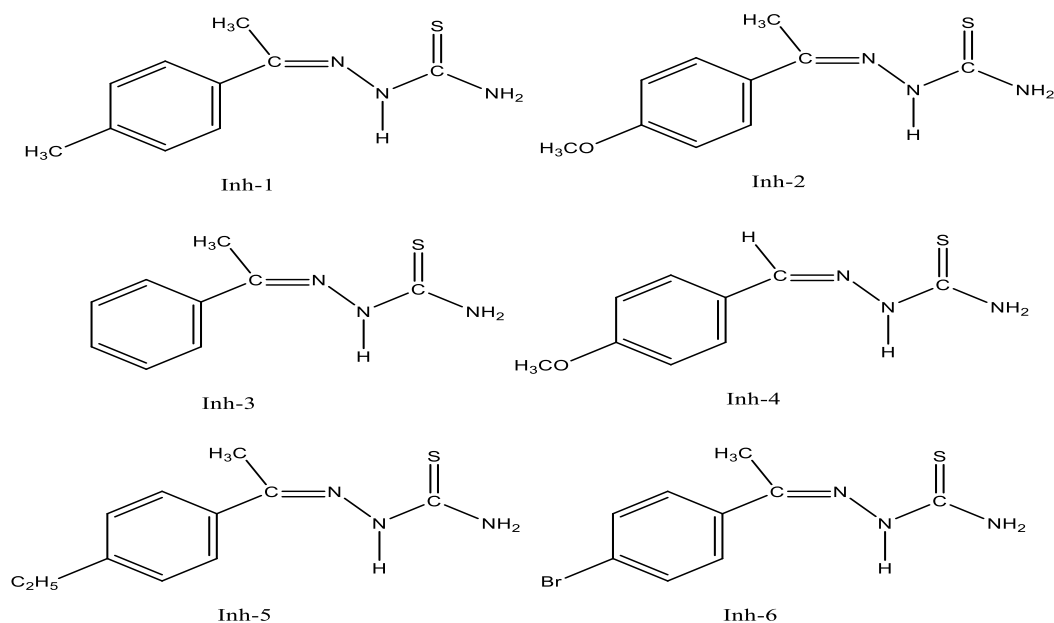

Figure 1. Chemical structures of examined thiosemicarbazone derivatives.

2. COMPUTATIONAL DETAILS

2.1. Calculation Method

Gaussian package program was used for all calculations such as the gradient-corrected correlation functional of Lee-Yang-Parr (B3LYP) [44] functional, combining Becke's 1988 exchange

functional with the correlation functional by Lee, Yang, and Parr, in conjunction with the B3LYP/6-311++G(2d,2p) and 6-311++G(3df,3pd), cc-pVTZ basic sets. Basic sets improved by Dunning and co-workers [45] are designed to converge systematically to the complete basis set (CBS) limit by using empirical extrapolation techniques. The cc-p, stands for correlation-consistent polarized and the V indicates they are valence-only basic sets. BP86 [46] which is composed of the Becke 1988 exchange functional and the Perdew 86 correlation functional and Restricted Hartree-Fock (RHF) methods in conjunction with the 6-311++G(2d,2p) basis set also were used to perform all the studied calculations. The mentioned calculations were performed in the gas and water medium in neural and protonated forms.

2.2. Definitions and Equations

Quantum chemical parameters like chemical hardness (η), chemical potential (μ) and electronegativity (χ) can be considered as measures of electron donating or accepting capabilities of chemical compounds [42-49]. In the Conceptual Density Functional Theory (CDFT) [50,51] that provided important contributions to the development of quantum chemistry, aforementioned quantum chemical parameters are described as below as the derivative of electronic energy (E) with respect to number of electron (N) at a constant external potential $v(r)$.

$$\chi = -\mu = -\left(\frac{\partial E}{\partial N}\right)_{v(r)} \tag{1}$$

$$\eta = \frac{1}{2}\left(\frac{\partial \mu}{\partial N}\right)_{v(r)} = \frac{1}{2}\left(\frac{\partial^2 E}{\partial N^2}\right)_{v(r)} \tag{2}$$

It is seen from the Eq. 1, electronegativity is given as the negative of the chemical potential. To calculate approximately the chemical hardness, chemical potential and electronegativity, Pearson and Parr applied the finite differences approach [52] to the mathematical definitions given above and presented the following equations based on ground state ionization energy (I) and electron affinity (A) values of chemical species such as atom, ion or molecule to calculate aforementioned parameters. Here, it is important to note that softness (σ) that can be considered as a measure of the polarizability is the multiplicative inverse of chemical hardness (η).

$$I = -E_{HOMO} \tag{3}$$

$$A = -E_{LUMO} \tag{4}$$

$$\eta = \frac{I-A}{2} \tag{5}$$

$$\sigma = \frac{1}{\eta} \tag{6}$$

$$\chi = -\mu = \frac{I+A}{2} \tag{7}$$

I and A of molecules can be calculated with the help of Koopmans theorem [53,54]. According to this theorem, the negative value of E_{HOMO} and E_{LUMO} corresponds to ionization energy and electron affinity, respectively. In that case, hardness, chemical potential and electronegativity can be calculated with the help of the following equations:

$$\mu = -\chi \cong \frac{E_{HOMO} + E_{LUMO}}{2} \tag{8}$$

$$\eta = \frac{E_{LUMO} - E_{HOMO}}{2} \tag{9}$$

As is known, the most applicable acid-base definition is Lewis acid-base definition. Lewis acid-base definition describes a base as electron pair donor. It should be noted that there is a significant correlation and proton affinity. Proton affinity [55] also is an important parameters used to predict inhibition efficiencies of chemical compounds. Although some authors pointed out that proton affinity is the negative of electronegativity, we calculated proton affinity of studied molecules considering following formulas.

$$PA = E_{(pro)} - \left(E_{(non-pro)} + E_{(H^+)} \right) \qquad (10)$$

where, $E_{non-pro}$ is the energies of the non-protonated and E_{pro} is the energies protonated Inhibitors, E_{H^+} is the energy of H^+ ion and was calculated as:

$$E_{(H^+)} = E_{(H_3O^+)} - E_{(H_2O)} \qquad (11)$$

According to Parr and co-workers [56], global molecular electrophilicity (ω) and global molecular nucleophilicity (ε) index can be calculated based on molecular electronegativity and molecular hardness values of studied compounds with the help of the following equations, respectively.

$$\omega = \frac{\chi^2}{2\eta} \qquad (12)$$

$$\varepsilon = \frac{1}{\omega} \qquad (13)$$

3. RESULTS AND DISCUSSION

Quantum chemical calculations and molecular modelling techniques are widely considered to characterize the molecules in terms of reactivity shape and binding properties [57,58]. Quantum chemical parameters like ionization energy, electron affinity, E_{HOMO} and E_{LUMO}, chemical hardness and softness, dipole moment, proton affinity, electronegativity, electrophilicity and nucleophilicity are very useful and provide important hints to predict theoretically the inhibition efficiencies of molecules.

According to the frontier molecular orbital theory (FMO), the chemical reactivity of molecule is a function of interaction between HOMO and LUMO levels of the reacting species [36]. HOMO and LUMO are known as frontier orbitals, and these energies of a molecule play important role in the determination of its molecular reactivity or stability. E_{HOMO} and E_{LUMO} are very widely used parameters associated with electron donating and electron accepting ability of molecules, respectively. HOMO orbital includes the electrons having high energy and acts as an electron donor orbital. On the other hand, LUMO act is an electron acceptor orbital [59,60]. It's important to note that the corrosion inhibition performances of molecules can be predicted in the light of the energies of aforementioned orbitals. Frontier Molecular orbital theory states that a molecule with high E_{HOMO} value acts a good corrosion inhibitor giving the electrons to metal surface. On the other hand, E_{LUMO} is associated with electron accepting ability of a molecule, and a molecule having low E_{LUMO} value cannot act a good corrosion inhibitor and it is ineffective against the corrosion of metal surfaces.

The optimized molecular structures HOMOs, LUMOs and total electron density are also given in Figure 2 for gas phase by using DFT/B3LYP/6-311++G(2d,2p) basic set. From the Figure 2, it could be seen that Inh 1 and Inh 2, 3 and Inh 6; 4 and Inh 5 have similar HOMO and LUMO distributions. The HOMO and LUMO of molecules Inh 1-6 are mainly located around the C=S moiety.
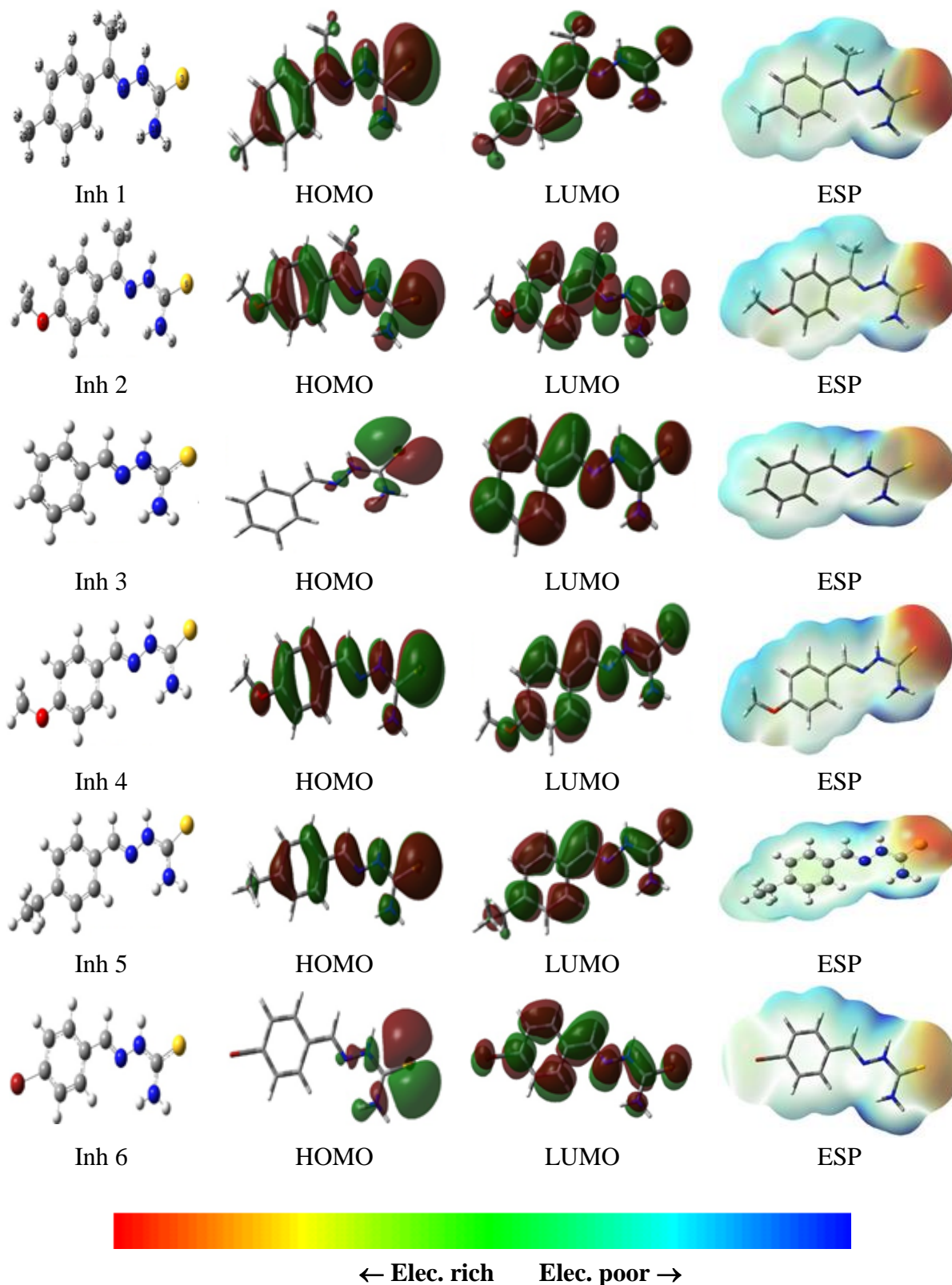
Figure 2. The optimized molecular structures for gas phase.

The presence of sulfur atoms together with several *p*-electrons on these molecules to be causes strong adsorption of the inhibitors on the steel surface. Also, this figure shows that there is much more

electron density in the vicinity of sulfur atoms for all studied molecules. The results show that adsorption of molecules on the metal surface with C = S bond is easier. Obi-Egbedi and et al. showed that the C = S bond with the metal surface adsorbed more easily [61].

In supplementary Tables S1-5, calculated quantum chemical parameters are presented for studied molecules and their gas and water medium in neural and protonated forms. At this stage, we should give some explanations about labelling in the supplementary tables. w and p symbols represent the water phase and protonation process. For instance, the label of Inh 2w-1p shows that Inh 2 is protonated on the nitrogen atom numbered 1 in water phase. The label of Inh 1-Sp means that Inh 1 is protonated on the sulfur atom in the gas phase. The schematic representation of studied compounds is given via Figure 3. In this figure, the number and the places of nitrogen and sulfur heteroatoms are showed clearly. E_{HOMO} values of Inh 1-6 molecules were found for gas phase -5.819, -5.709, -5.955, -5.735, -5.682, -9.062 eV by using DFT/B3LYP/6-311++G(2d,2p) basic set, respectively (supplementary Table S1). According to these results, the electron donating trends for study molecules for gas can be written as: Inh 1>Inh 2 for acetophenone thiosemicarbazone compounds, and Inh 6>Inh 3>Inh 5>Inh 4 for benzaldehyde thiosemicarbazone and its *p*-substituted derivatives. E_{HOMO} and E_{LUMO} values in Inh 2 for acetophenone thiosemicarbazone compounds and Inh 4 for benzaldehyde thiosemicarbazone and its *p*-substituted derivatives molecules are lower than other molecules. This is due to the methoxy group attached to the phenyl ring of Inh 2 and Inh 4 molecules. As is known, the methoxy group is an electron attracting group. Considering the information given above about HOMO-LUMO energy levels and their relationships with corrosion inhibition efficiency, inhibition efficiencies of investigated molecules obey the order: Inh 2>Inh 1 for acetophenone thiosemicarbazone compounds and Inh 4>Inh 5>Inh 3>Inh 6 for benzaldehyde thiosemicarbazone and its *p*-substituted derivatives. This result is in good agreement with experimental data obtained by Arab and Emran [29].
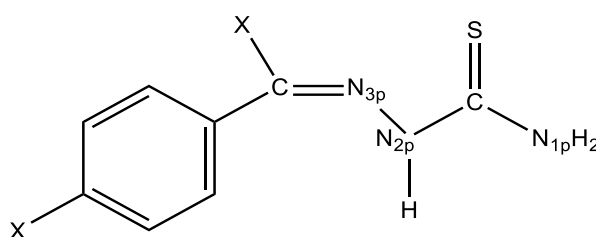

Figure 3. Schematic representation of studied compounds.

Chemical hardness, softness and ΔE are closely interrelated chemical properties [61-63]. Chemical hardness introduced in 1960s by Pearson [64] is defined as the resistance towards electron cloud polarization or deformation of chemical species. According to the Maximum Hardness Principle states; "a chemical system tends to arrange itself so as to achieve maximum hardness and chemical hardness can be considered as a measurement of stability" [65]. Pearson showed that hard molecules with a high ΔE values are more stable compared to soft molecules with a low ΔE values. ΔE values of Inh 1-6 molecules were found for gas phase by using DFT/B3LYP/6-311++G(2d,2p) basic set 4.047, 4.055, 3.822, 3.862, 3.835, 3.724 eV, respectively (supplementary Table S1). Inh 2 molecule is found

more stable than other molecule Inh 1, and Inh 4 is found more stable than other benzaldehyde thiosemicarbazone and its *p*-substituted derivatives molecules for gas phase due to the fact that a large ΔE value is observed. The softness is a measure of the polarizability of chemical species. Soft molecules give easily the electrons to metal surface and as act good corrosion inhibitors. Adsorption of inhibitor onto a metallic surface occurs in the part of a molecule having the greatest softness and lowest hardness [66]. Hasanov et. al. stated that softness is a local property and adsorption could occur at the part of the molecule where softness has a highest value [67]. The calculations indicate that Inh 2 among acetophenone thiosemicarbazone compounds, Inh 4 among benzaldehyde thiosemicarbazone and its *p*-substituted derivatives have lower chemical hardness values compared to the others. In the light of calculated quantum chemical parameters, such as E_{HOMO}, E_{LUMO}, hardness, softness and HOMO-LUMO energy gap values presented in supplementary Tables S1-4 for studied compounds. The corrosion inhibition efficiency rankings can be written as Inh 2>Inh 1 for acetophenone thiosemicarbazone compounds and Inh 4>Inh 5>Inh 3>Inh 6 for benzaldehyde thiosemicarbazone and its *p*-substituted derivatives. These rankings also are very compatible with experiments made.

Electronegativity that is defined as the electron attracting power of chemical species is a key parameter in corrosion studies and is widely used in the prediction of Inhibitive properties of molecules [68]. According to Sanderson's "electronegativity equalization principle" [69] when a metal and an inhibitor come closer to each other, electrons flow from inhibitor with having a low electronegativity value to metal with having a higher electronegativity value, until their chemical potentials or electronegativities become equal. It can be easily understood from this expression, the electronegativity of inhibitor molecule determines the fraction of electrons transferred from the inhibitor to metal surface. A good corrosion inhibitor has low electronegativity value. From supplementary Table S2, it is possible to observe that 3.944, 3.682, 4.044, 3.805, 3.944 and 4.199 eV by using B3LYP/6-311++G(2d,2p) basic set and 3.834, 3.308, 4.049, 3.341, 3.962 and 4.191 eV by using BP86/6-311++G(2d,2p) basic set for molecules 1-6 in gas phase, respectively. The order of electronegativity follows the trend Inh 2<Inh 1 for acetophenone thiosemicarbazone compounds and Inh 4<Inh 5<Inh 3<Inh 6 for benzaldehyde thiosemicarbazone and its *p*-substituted derivatives, which are agreement with experimental data. The same trend is seen in other basic sets as well for in gas and water phase of neutral and protonated forms of molecules by using different methods and basis sets (see supplementary Tables S1-4).

Proton affinity (PA) is defined as the enthalpy change of the reaction with hydrogen ion of a chemical species in the gas phase. This quantity that is a measure of the basicity and it is provides important clues about electron donating or accepting abilities of compounds [55]. Organic molecules including nitrogen and sulfur heteroatoms like thiosemicarbazone derivatives have high tendency to protonation in acidic media and aqueous solution. Therefore, we analyzed the both neutral and protonated forms of studied compounds to predict their proton affinities using Eq. 10 and 11. Kaya et. al. reported that corrosion inhibition efficiency increases as the negative value of proton affinity increases [70]. PA values of investigational molecules Inh 1-6 for gas phase were found by using three methods and the results: -2.287, -2.361, -2.145, -2.322, -2.231, -2.073 eV with B3LYP/6311++G(2d,2p) method, respectively (PA results of the other methods for gas and water phase of neutral and protonated forms of molecules phase can be seen in supplementary Tables S2 and S4). The results obtained showed that the corrosion inhibition efficiency rankings for studied compounds in terms of the proton affinity

values can be given as: Inh 2>Inh 1 for acetophenone thiosemicarbazone compounds and Inh 4>Inh 5>Inh 3>Inh 6 for benzaldehyde thiosemicarbazone and its *p*-substituted derivatives. This further supports the experimental results.

Recently, some authors calculated and used electrophilicity (ω) and nucleophilicity (ε) indexes of molecules in corrosion studies and noted that these indexes are useful theoretical descriptors in the prediction of Inhibitive performances of molecules against the corrosion of metal surfaces [71,72]. Parr's electrophilicity index is based on chemical hardness and electronegativity values of molecules as given in Eq. 12 and nucleophilicity is generally given as the multiplicative inverse of the electrophilicity. It is apparent that molecules having high electrophilicity values are ineffective to prevent the corrosion of metal. A good corrosion inhibitor has low electrophilicity or high nucleophilicity value. It can be seen from the tables including the calculated quantum chemical parameters that predicted corrosion inhibition efficiency rankings can be given as: Inh 2>Inh 1 for acetophenone thiosemicarbazone compounds and Inh 4>Inh 5>Inh 3>Inh 6 for benzaldehyde thiosemicarbazone and its *p*-substituted derivatives. The electrophilicity values of Inh 1-6 for gas phase were found by using B3LYP/6311++G(2d,2p) method and the results: 3.561, 3.342, 4.278, 3.748, 4.055, 4.732 eV, respectively. These rankings also are very compatible with experimentally observed results.

Dipole moment (D) is another indicator of corrosion inhibition efficiencies of chemical compounds. Although some authors reported that there is no any remarkable relationship between dipole moment and inhibition efficiency, several authors showed that corrosion inhibition efficiency increases with the increasing of the dipole moment [35]. In some studies, authors supported that increasing value of dipole moment facilitates the electron transport process [73,74]. Here, our calculated dipole moment values are in good agreement with experimental corrosion inhibition efficiencies. For instance, in supplementary Table S2, calculated dipole moment values for molecules Inh 1-6 by 6-311++G(2d,2p) method for gas phase are 6.011, 7.027, 5.405, 7.132, 6.243 and 3.441, respectively. It is apparent that this data given is very compatible with experimental results. Namely, our calculations can be considered a new support for the relation between dipole moment with inhibition efficiency.

As can be seen from calculations made and electrostatic potential structures given in Figure 2, the most suitable region for the protonation of studied thiosemicarbazone derivatives is on the sulfur atom (red colour). In such studies, electronic charge analysis for atoms in the molecules is important because binding capability of a molecule depends also on electronic charge on heteroatoms of the molecule. The binding facilitates as the negative charge on heteroatom increases [58]. In the study, to calculate the atomic charges we used Mulliken population analysis [75]. In supplementary Table S5, calculated Mulliken charges on sulfur atom in studied molecules using some calculation levels are given. It can be seen from the mentioned table, Mulliken charges calculated also are very compatible with experimental inhibition efficiencies.

4. CONCLUSIONS

In this computational study, using some calculation levels that are widely considered in corrosion studies, we investigated a correlation between electronic structure parameters like frontier orbital energies, hardness, softness, HOMO-LUMO energy gap, dipole moment, electronegativity, proton affinity, electrophilicity, nucleophilicity, Mulliken charges and experimental inhibition efficiencies of

some thiosemicarbazone derivatives (Inh 1-6). Most of the calculated parameters using B3LYP/6311++G(2d,2p), B3LYP/cc-pVTZ and BP86/6-311++G(2d,2p) calculation levels for neutral and protonated forms of mentioned molecules show excellent agreement with experimental data confirming the reliability of the calculation levels employed. From the theoretical data, the inhibitive performances of studied compounds obey the order: Inh 2>Inh 1 for acetophenone thiosemicarbazone compounds and Inh 4>Inh 5>Inh 3>Inh 6 for benzaldehyde thiosemicarbazone and its *p*-substituted derivatives and these rankings agree well with experiment.

References

1. I. B. Obot, S. Kaya, C. Kaya, B. Tüzün, *Physica E.*, 80 (2016) 82.
2. I. B. Obot, N. O. Obi-Egbedi, *Corros. Sci.*, 52 (2010) 198.
3. E. E. Ebenso, T. Arslan, F. Kandemirli, I. Love, C. Öğretir, M. Saraçoğlu, S. A. Umoren, *Int. J. Quant. Chem.*, 110 (2010) 2614.
4. M. A. Amin, M. A. Ahmed, H. A. Arida, T. Arslan, M. Saraçoğlu, F. Kandemirli, *Corros. Sci.*, 53 (2011) 540.
5. K. F. Khaled, *Electrochim. Acta*, 48 (2003) 2493.
6. P. Shing, E. E. Ebenso, L. O. Olasunkanmi, I. B. Obot, M. A. Quraishi, *J. Phys. Chem. C.*, 120 (2016) 3408.
7. K. S. Jacob, G. Parameswaran, *Corros. Sci.*, 52 (2010) 224.
8. M. M. Solomon, S. A. Umoren, I. I. Udosoro, A. P. Udoh, *Corros. Sci.*, 52 (2010) 1317.
9. J. Stringer, ASM International, High Temperature Corrosion and Materials Application, Hot Corrosion in Gas Turbines, 9 (2007) 249.
10. B. O. Hasan, S. A. Sadek, *Adv. Chem. Eng. Res.*, 2 (2013) 61.
11. W. Huybregts, *Mater. Perform.*, 16 (1977) 23.
12. G. Mrowczynski, Z. Szklarska-Smialowska, *J. Appl. Electrochem.*, 9 (1979) 201.
13. E. S. H. El Ashry, A. El Nemr, S. A. Esawy, S. Ragab, *Electrochim. Acta*, 51 (2006) 3957.
14. P. Zhao, Q. Lyang, Y. Li, *Appl. Surf. Sci.*, 252 (2005) 1596.
15. A. Yurt, S. Ulutas, H. Dal, *Appl. Surf. Sci.*, 253 (2006) 919.
16. Y. Xiao-Ci, Z. Hong, L. Ming-Dao, R. Hong-Xuan, Y. Lu-An, *Corros. Sci.*, 42 (2000) 645.
17. D. Wang, S. Li, Y. Ying, M. Wang, H. Xiao, Z. Chen, *Corros. Sci.*, 41 (1999) 1911.
18. F. Kandemirli, S. Sağdınç, *Corros. Sci.*, 49 (2007) 2118.
19. S. Zor, M. Saraçoğlu, F. Kandemirli, T. Arslan, *Corrosion*, 67 (2011) 125003-1.
20. M. A. Amin, M. A. Ahmed, H. A. Arida, F. Kandemirli, M. Saracoglu, T. Arslan, M. A. Basaran, *Corros. Sci.*, 53 (2011) 1895.
21. E. E. Ebenso, M. M. Kabanda, T. Arslan, M. Saracoglu, F. Kandemirli, L. C. Murulana, A. K. Singh, S. K. Shukla, B. Hammouti, K. F. Khaled, M. A. Quraishi, I. B. Obot, N. O. Edd, *Int. J. Electrochem. Sci.*, 7 (2012) 5643.
22. M. A. Amin, O. A. Hazzazi, F. Kandemirli, M. Saracoglu, *Corrosion*, 68 (2012) 688.
23. F. Kandemirli, M. Saracoglu, M. A. Amin, M. A. Basaran, C. D. Vurdu, *Int. J. Electrochem. Sci.*, 9 (2014) 3819.
24. M. A. Amin, N. El-Bagoury, M. Saracoglu, M. Ramadan, *Int. J. Electrochem. Sci.*, 9 (2014) 5352.
25. N. El-Bagoury, M. A. Amin, M. Saracoglu, *Int. J. Electrochem. Sci.*, 10 (2015) 5291.
26. M. A. Amin, S. A. Fadlallah, G. S. Alosaimi, F. Kandemirli, M. Saracoglu, S. Szunerits, R. Boukherroub, *Int. J. Hydrogen Energy*, 41 (2016) 6326.
27. A. Tazouti, M. Galai, R. Touir, M. Ebn Touhami, A. Zarrouk, Y. Ramli, M. Saraçoğlu, S. Kaya, F. Kandemirli, C. Kaya, *J. Mol. Liquids*, 221 (2016) 815.

28. M. A. Amin, M. Saracoglu, N. El-Bagoury, T. Sharshar, M. M. Ibrahim, J. Wysocka, S. Krakowiak, J. Ryl, *Int. J. Electrochem. Sci.*, 11 (2016) 10029.
29. S. T. Arab, K. M. Emran, *Mater. Lett.*, 62 (2008) 1022.
30. G. Gece, *Corros. Sci.*, 50 (2008) 298.
31. G. Bereket, C. Ogretir, A. Yurt, *J. Mol. Struct.*, 571 (2001) 13.
32. M. K. Awad, *J. Electroanal. Chem.*, 567 (2004) 219.
33. M. K. Awad, F. M. Mahgoub, M. M. El-iskandrani, *J. Mol. Struct.*, 531 (2000) 105.
34. I. B. Obot, N. O. Obi-Egbedi, *Corros. Sci.*, 52 (2010) 657.
35. G. Gao, C. Liang, *Electrochim. Acta*, 52 (2007) 4554.
36. A. Y. Musa, A. H. Kadhum, A. B. Mohamad, A. B. Rohoma, H. Mesmari, *J. Mol. Struct.*, 969 (2010) 233.
37. H. Ju, Z. Kai, Y. Li, *Corros. Sci.*, 50 (2008) 865.
38. E. E. Ebenso, D. A. Isabirye, N. O. Eddy, *Int. J. Mol. Sci.*, 11 (2010) 2473.
39. T. Arslan, F. Kandemirli, E. E. Ebenso, I. Love, H. Alemu, *Corros. Sci.*, 51 (2009) 35.
40. M. Ozcan, *J. Solid State Electrochem.*, 12 (2008) 1653.
41. S. Zor, F. Kandemirli, M. Bingul, *Prot. Met. Phys. Chem. Surf.*, 45 (2009) 46.
42. D. Q. Zhang, Q. R. Cai, L. X. Gao, K.Y . Lee, *Corros. Sci.*, 50 (2008) 3615.
43. M. J. Frisch, G. W. Trucks, H. B. Schlegel, G. E. Scuseria, M. A. Robb, J. R. Cheeseman Jr., J. A. Montgomery, T. Vreven, K. N. Kudin, J. C. Burant, J. M. Millam, S. S. Iyengar, J. Tomasi, V. Barone, B. Mennucci, M. Cossi, G. Scalmani, N. Rega, G. A. Petersson, H. Nakatsuji, M. Hada, M. Ehara, K. Toyota, R. Fukuda, J. Hasegawa, M. Ishida, T. Nakajima, Y. Honda, O. Kitao, H. Nakai, M. Klene, X. Li, J. E. Knox, H. P. Hratchian, J. B. Cross, V. Bakken, C. Adamo, J. Jaramillo, R. Gomperts, R. E. Stratmann, O. Yazyev, A. J. Austin, R. Cammi, C. Pomelli, J. W. Ochterski, P. Y. Ayala, K. Morokuma, G. A. Voth, P. Salvador, J. J. Dannenberg, V. G. Zakrzewski, S. Dapprich, A. D. Daniels, M. C. Strain, O. Farkas, D. K. Malick, A. D. Rabuck, K. Raghavachari, J. B. Foresman, J. V. Ortiz, Q. Cui, A. G. Baboul, S. Clifford, J. Cioslowski, B. B. Stefanov, G. Liu, A. Liashenko, P. Piskorz, I. Komaromi, R.L. Martin, D. J. Fox, T. Keith, M. A. Al-Laham, C. Y. Peng, A. Nanayakkara, M. Challacombe, P. M. W. Gill, B. Johnson, W. Chen, M. W. Wong, C. Gonzalez, J. A. Pople, Gaussian 03W, Gaussian Inc., Wallingford, CT, 2004.
44. P. J. Stephens, F. J. Devlin, C. F. Chabalowski, M. J. Frisch, *J. Phys. Chem.*, 98 (1994) 11623.
45. T. H. Dunning, *J. Chem. Phys.*, 90 (1989) 1007.
46. A. D. Becke, *Phys. Rev. A.*, 38 (1988), 3098.
47. S. Kaya, C. Kaya, *Mol. Phys.*, 113 (2015) 1311.
48. S. Kaya, C. Kaya, *Comput. Theor. Chem.*, 1052 (2015) 42.
49. S. Kaya, C. Kaya, *Comput. Theor. Chem.*, 1060 (2015) 66.
50. F. De Proft, V. Forquet, B. Ourri, H. Chermette, P. Geerlings, C. Morell, *Phys. Chem. Chem. Phys.*, 17 (2015) 9359.
51. P. Geerlings, F. De Proft, W. Langenaeker, *Chem. Rev.*, 103 (2003) 1793.
52. R. G. Pearson, *Inorg. Chem.*, 27 (1988) 734.
53. T. Koopmans, *Physica.*, 1 (1933) 104.
54. S. Kaya, L. Guo, C. Kaya, B. Tüzün, I. B. Obot, R. Touir, N. Islam, *J. Taiwan Int. Chem. Eng.*, 65 (2016) 522.
55. B. J. Smith, L. Radom, *J. Phys. Chem.*, 99 (1995) 6468.
56. R. G. Parr, L. V. Szentpaly, S. Liu, *J. Am. Chem. Soc.*, 121 (1999) 1922.
57. G. Gece, *Corros. Sci.*, 50 (2008) 2981.
58. G. Gece, S. Bilgiç, *Corros. Sci.*, 51 (2009) 1876.
59. A. Popova, M. Christov, T. Deligeorgiev, *Corrosion*, 59 (2003) 756.
60. R. Yıldız, *Corros. Sci.*, 90 (2015) 544.
61. N. O. Obi-Egbedi, I. B. Obot, M. I. El-Khaiary, *J. Mol. Struct.*, 1002 (2011) 86.
62. I. B. Obot, N. O. Obi-Egbedi, A. O. Eseola, *Ind. Eng. Chem. Res.*, 50 (2011) 2098.

63. I. B. Obot, N. O. Obi-Egbedi, E. E. Ebenso, A. S. Afolabi, E. E. Oguzie, *Res. Chem. Intermed.*, 39 (2012) 1927.
64. R. G. Pearson, *J. Am. Chem. Soc.*, 85 (1963) 3533.
65. R. G. Parr, P. K. Chattaraj, *J. Am. Chem. Soc.*, 113 (1991) 1854.
66. L. Guo, S. Zhu, S. Zhang, Q. He, W. Li, *Corros. Sci.*, 87 (2014) 366.
67. R. Hasanov, M. Sadıkoglu, S. Bilgiç, *Appl. Surf. Sci.*, 253 (2007) 3913.
68. E. E. Ebenso, *Mater. Chem. Phys.*, 79 (2003) 58.
69. S. Kaya, C. Kaya, N. Islam, *Comput. Theor. Chem.*, 1080 (2016) 72.
70. S. Kaya, C. Kaya, L. Guo, F. Kandemirli, B. Tüzün, İ. Uğurlu, M. Saraçoğlu, *J. Mol. Liq.*, 219 (2016) 497.
71. S. Kaya, P. Banerjee, S. K. Saha, B.Tüzün, C. Kaya, *RSC Adv.*, 6 (2016) 74550.
72. A. Tazouti, M. Galai, R. Touir, M. Ebn Touhami, A. Zarrouk, Y. Ramli, M. Saraçoğlu, S. Kaya, F. Kandemirli, C. Kaya, *J. Mol. Liq.*, 221 (2016) 815.
73. M. Sahin, G. Gece, F. Karci, S. Bilgic, *J. Appl. Electrochem.*, 38 (2008) 809.
74. M. A. Quraishi, R. Sardar, *J. Appl. Electrochem.*, 33 (2003) 1163.
75. J. N. Murrell, S. F. Kettle, J. M. Tedder, The Chemical Bond, (1985) John Wiley & Sons, Chichester, UK.

SUPPLEMENTARY INFORMATION

Table S1. The calculated quantum chemical parameters, HOMO, LUMO, ΔE for the non-protonated for gas and solvent phase compounds by using B3LYP/6-311++G(2d,2p), B3LYP/cc-pVTZ and BP86/6-311++G(2d,2p) methods.

Mol.	E_{HOMO}, eV	E_{LUMO}, eV	ΔE, eV	Mol.	E_{HOMO}, eV	E_{LUMO}, eV	ΔE, eV
B3LYP/6311++G(2d,2p)							
Inh 1	-5.819	-1.773	4.047	Inh 1-w	-6.122	-1.788	4.334
Inh 2	-5.709	-1.654	4.055	Inh 2-w	-5.962	-1.709	4.252
Inh 3	-5.955	-2.133	3.822	Inh 3-w	-6.220	-2.064	4.156
Inh 4	-5.735	-1.874	3.862	Inh 4-w	-5.970	-1.875	4.095
Inh 5	-5.862	-2.026	3.835	Inh 5-w	-6.138	-1.992	4.146
Inh 6	-6.062	-2.336	3.726	Inh 6-w	-6.233	-2.184	4.049
B3LYP/cc-pVTZ							
Inh 1	-5.728	-1.651	4.076	Inh 1-w	-6.049	-1.665	4.385
Inh 2	-5.615	-1.517	4.098	Inh 2-w	-5.886	-1.572	4.314
Inh 3	-5.855	-1.997	3.859	Inh 3-w	-7.021	-1.940	5.080
Inh 4	-5.640	-1.729	3.911	Inh 4-w	-5.894	-1.739	4.155
Inh 5	-5.773	-1.898	3.875	Inh 5-w	-6.065	-1.871	4.195
Inh 6	-5.968	-2.210	3.757	Inh 6-w	-6.158	-2.069	4.089
BP86/6-311++G(2d,2p)							
Inh 1	-5.113	-2.555	2.558	Inh 1-w	-5.433	-2.592	2.841
Inh 2	-4.191	-2.426	1.765	Inh 2-w	-5.272	-2.500	2.772
Inh 3	-5.224	-2.875	2.348	Inh 3-w	-5.545	-2.844	2.701
Inh 4	-5.074	-2.608	2.466	Inh 4-w	-5.300	-2.645	2.655
Inh 5	-5.157	-2.768	2.389	Inh 5-w	-5.470	-2.771	2.699
Inh 6	-5.327	-3.054	2.273	Inh 6-w	-5.557	-2.945	2.612

w: water phase

Table S2. The calculated other quantum chemical parameters for the non-protonated for gas and solvent phase compounds by using B3LYP/6-311++G(2d,2p), B3LYP/cc-pVTZ and BP86/6-311++G(2d,2p) methods.

Mol.	η, eV	σ, eV^{-1}	χ, eV	PA, eV	ω, eV	ε, eV^{-1}	D, Debye	Energy, eV
B3LYP/6311++G(2d,2p)								
Inh 1	2.023	0.494	3.796	-2.287	3.561	0.281	6.011	-25888.109
Inh 2	2.028	0.493	3.682	-2.361	3.342	0.299	7.027	-27935.155
Inh 3	1.911	0.523	4.044	-2.145	4.278	0.234	5.405	-23749.084
Inh 4	1.931	0.518	3.805	-2.322	3.748	0.267	7.132	-26865.711
Inh 5	1.918	0.521	3.944	-2.231	4.055	0.247	6.243	-25888.032
Inh 6	1.863	0.537	4.199	-2.073	4.732	0.211	3.441	-93779,538
B3LYP/cc-pVTZ								
Inh 1	2.038	0.491	3.689	-2.356	3.339	0.299	5.843	-25888.991
Inh 2	2.049	0.488	3.566	-2.184	3.104	0.322	6.894	-27936.140
Inh 3	1.929	0.518	3.926	-2.217	3.994	0.250	5.299	-23749.878
Inh 4	1.956	0.511	3.685	-2.398	3.471	0.288	7.000	-26866.653
Inh 5	1.938	0.516	3.836	-2.300	3.796	0.263	6.053	-25888.922
Inh 6	1.879	0.532	4.089	-2.144	4.450	0.225	3.335	-93782.703
BP86/6-311++G(2d,2p)								
Inh 1	1.279	0.782	3.834	-2.259	5.745	0.174	5.559	-25888.924
Inh 2	0.882	1.133	3.308	-2.360	6.201	0.161	6.741	-27936.102
Inh 3	1.174	0.852	4.049	-2.112	6.984	0.143	4.882	-23749.968
Inh 4	1.233	0.811	3.841	-2.324	5.982	0.167	6.820	-26866.678
Inh 5	1.195	0.837	3.962	-2.210	6.571	0.152	5.761	-25888.808
Inh 6	1.137	0.880	4.191	-2.005	7.726	0.129	3.002	-93787.381
B3LYP/6311++G(2d,2p)								
Inh 1-w	2.167	0.461	3.955	-3.877	3.610	0.277	8.775	-25888.524
Inh 2-w	2.126	0.470	3.835	-3.886	3.460	0.289	10.014	-27935.621
Inh 3-w	2.078	0.481	4.142	-3.892	4.129	0.242	8.072	-23749.480
Inh 4-w	2.048	0.488	3.922	-3.873	3.757	0.266	10.181	-26866.167
Inh 5-w	2.073	0.482	4.065	-3.868	3.986	0.251	9.115	-25888.436
Inh 6-w	2.025	0.494	4.208	-3.895	4.374	0.229	5.542	-93779.952
B3LYP/cc-pVTZ								
Inh 1-w	2.192	0.456	3.857	-3.950	3.393	0.295	8.512	-25889.403
Inh 2-w	2.157	0.464	3.729	-3.955	3.223	0.310	9.797	-27936.599
Inh 3-w	2.540	0.394	4.480	-3.945	3.951	0.253	7.874	-23750.274
Inh 4-w	2.078	0.481	3.816	-3.939	3.505	0.285	9.981	-26867.110
Inh 5-w	2.097	0.477	3.968	-3.928	3.753	0.266	8.819	-25889.325
Inh 6-w	2.044	0.489	4.114	-3.959	4.139	0.242	5.342	-93783.116
BP86/6-311++G(2d,2p)								
Inh 1-w	1.421	0.704	4.012	-3.840	5.667	0.176	8.369	-25889.320
Inh 2-w	1.386	0.722	3.886	-3.850	5.449	0.184	9.868	-27936.553
Inh 3-w	1.351	0.740	4.195	-3.769	6.515	0.153	7.528	-23750.359
Inh 4-w	1.328	0.753	3.972	-3.842	5.944	0.168	10.061	-26867.138
Inh 5-w	1.349	0.741	4.120	-3.808	6.290	0.159	8.686	-25889.206
Inh 6-w	1.306	0.766	4.251	-3.807	6.918	0.145	5.061	-93787.740

w: water phase

Table S3. The calculated quantum chemical parameters, HOMO, LUMO, ΔE for the protonated for gas and solvent phase compounds by using B3LYP/6-311++G(2d,2p), B3LYP/cc-pVTZ and BP86/6-311++G(2d,2p) methods.

Mol.	E_{HOMO}, eV	E_{LUMO}, eV	ΔE, eV	Mol.	E_{HOMO}, eV	E_{LUMO}, eV	ΔE, eV
			B3LYP/6-311++G(2d,2p)				
Inh 1-1p	-9.747	-6.065	3.682	Inh 1-1pw	-6.082	-3.525	2.557
Inh 2-1p	-9.261	-5.922	3.339	Inh 2-1pw	-5.769	-3.452	2.317
Inh 3-1p	-10.121	-6.274	3.847	Inh 3-1pw	-6.269	-3.646	2.623
Inh 4-1p	-9.355	-5.950	3.405	Inh 4-1pw	-5.814	-2.428	3.386
Inh 5-1p	-9.781	-6.112	3.669	Inh 5-1pw	-6.119	-3.582	2.537
Inh 6-1p	-9.790	-6.330	3.460	Inh 6-1pw	-6.207	-3.705	2.502
Inh 1-1p	-10.218	-5.778	4.440	Inh 1-1pw	-6.508	-3.253	3.255
Inh 2-1p	-9.652	-5.619	4.032	Inh 2-1pw	-6.093	-3.144	2.949
Inh 3-1p	-10.804	-6.328	4.476	Inh 3-1pw	-6.544	-3.597	2.946
Inh 4-1p	-9.857	-5.894	3.963	Inh 4-1pw	-6.157	-3.306	2.851
Inh 5-1p	-10.318	-6.003	4.315	Inh 5-1pw	-6.486	-3.471	3.015
Inh 6-1p	-10.251	-6.394	3.858	Inh 6-1pw	-6.552	-3.690	2.862
Inh 1-1p	-9.541	-6.698	2.844	Inh 1-1pw	-5.905	-4.030	1.875
Inh 2-1p	-9.335	-6.539	2.796	Inh 2-1pw	-5.865	-3.909	1.955
Inh 3-1p	-9.826	-7.162	2.664	Inh 3-1pw	-6.076	-4.173	1.903
Inh 4-1p	-9.301	-6.861	2.441	Inh 4-1pw	-5.860	-4.109	1.751
Inh 5-1p	-9.474	-7.100	2.374	Inh 5-1pw	-5.897	-4.327	1.570
Inh 6-1p	-9.803	-7.186	2.617	Inh 6-1pw	-6.086	-4.230	1.856
Inh 1-1p	-9.676	-5.830	3.847	Inh 1-1pw	-6.130	-3.188	2.942
Inh 2-1p	-9.167	-5.704	3.463	Inh 2-1pw	-5.768	-3.116	2.652
Inh 3-1p	-10.104	-5.928	4.176	Inh 3-1pw	-6.357	-3.354	3.003
Inh 4-1p	-9.304	-5.770	3.534	Inh 4-1pw	-5.818	-3.180	2.638
Inh 5-1p	-9.756	-5.844	3.912	Inh 5-1pw	-6.185	-3.290	2.895
Inh 6-1p	-9.696	-6.003	3.693	Inh 6-1pw	-6.261	-3.436	2.824
			B3LYP/cc-pVTZ				
Inh 1-1p	-9.727	-6.021	3.706	Inh 1-1pw	-6.673	-2.703	3.970
Inh 2-1p	-9.228	-5.869	3.359	Inh 2-1pw	-6.356	-2.646	3.710
Inh 3-1p	-10.098	-6.232	3.866	Inh 3-1pw	-6.846	-2.819	4.027
Inh 4-1p	-9.321	-5.899	3.422	Inh 4-1pw	-6.379	-2.674	3.705
Inh 5-1p	-9.761	-6.071	3.689	Inh 5-1pw	-6.687	-2.766	3.920
Inh 6-1p	-9.767	-6.288	3.478	Inh 6-1pw	-6.795	-2.896	3.899
Inh 1-1p	-10.197	-5.724	4.473	Inh 1-1pw	-7.197	-2.339	4.858
Inh 2-1p	-9.617	-5.548	4.069	Inh 2-1pw	-6.711	-2.244	4.468
Inh 3-1p	-10.758	-6.267	4.492	Inh 3-1pw	-7.331	-2.700	4.630
Inh 4-1p	-9.778	-5.730	4.048	Inh 4-1pw	-6.782	-2.418	4.364
Inh 5-1p	-10.296	-5.946	4.350	Inh 5-1pw	-7.191	-2.569	4.622
Inh 6-1p	-10.232	-6.335	3.897	Inh 6-1pw	-7.313	-2.822	4.492
Inh 1-1p	-9.504	-6.639	2.865	Inh 1-1pw	-6.625	-3.251	3.374
Inh 2-1p	-9.278	-6.478	2.800	Inh 2-1pw	-6.593	-3.140	3.453
Inh 3-1p	-9.758	-7.100	2.658	Inh 3-1pw	-6.772	-3.422	3.350
Inh 4-1p	-9.218	-6.811	2.408	Inh 4-1pw	-6.585	-3.340	3.244
Inh 5-1p	-9.412	-7.054	2.358	Inh 5-1pw	-6.625	-3.550	3.075
Inh 6-1p	-9.734	-7.125	2.609	Inh 6-1pw	-6.086	-4.230	1.856

Inh 1-1p	-9.638	-5.715	3.923	Inh 1-1pw	-6.751	-2.271	4.480
Inh 2-1p	-9.112	-5.588	3.524	Inh 2-1pw	-6.373	-2.173	4.200
Inh 3-1p	-10.070	-5.835	4.234	Inh 3-1pw	-6.985	-2.450	4.535
Inh 4-1p	-9.247	-5.658	3.589	Inh 4-1pw	-6.408	-2.274	4.134
Inh 5-1p	-9.721	-6.831	2.891	Inh 5-1pw	-6.790	-2.386	4.403
Inh 6-1p	-9.661	-5.914	3.747	Inh 6-1pw	-6.892	-2.557	4.335
BP86/6-311++G(2d,2p)							
Inh 1-1p	-9.146	-6.774	2.372	Inh 1-1pw	-6.705	-2.764	3.941
Inh 2-1p	-8.667	-6.591	2.077	Inh 2-1pw	-6.402	-2.713	3.689
Inh 3-1p	-9.529	-7.008	2.521	Inh 3-1pw	-6.880	-2.879	4.001
Inh 4-1p	-8.773	-6.629	2.144	Inh 4-1pw	-6.424	-2.737	3.686
Inh 5-1p	-9.197	-6.822	2.375	Inh 5-1pw	-6.718	-2.823	3.895
Inh 6-1p	-9.188	-7.020	2.168	Inh 6-1pw	-6.830	-2.952	3.878
Inh 1-1p	-9.554	-6.585	2.969	Inh 1-1pw	-7.226	-2.406	4.819
Inh 2-1p	-9.002	-6.387	2.615	Inh 2-1pw	-6.767	-2.323	4.445
Inh 3-1p	-9.961	-7.092	2.869	Inh 3-1pw	-7.378	-2.770	4.609
Inh 4-1p	-9.163	-6.551	2.612	Inh 4-1pw	-6.846	-2.540	4.306
Inh 5-1p	-9.646	-6.779	2.867	Inh 5-1pw	-7.225	-2.634	4.591
Inh 6-1p	-9.597	-7.102	2.495	Inh 6-1pw	-7.345	-2.886	4.459
Inh 1-1p	-8.827	-7.299	1.528	Inh 1-1pw	-6.701	-3.303	3.398
Inh 2-1p	-8.603	-7.119	1.484	Inh 2-1pw	-6.674	-3.199	3.475
Inh 3-1p	-9.140	-7.748	1.392	Inh 3-1pw	-6.847	-3.492	3.355
Inh 4-1p	-8.554	-7.450	1.105	Inh 4-1pw	-6.672	-3.399	3.273
Inh 5-1p	-8.810	-7.639	1.171	Inh 5-1pw	-6.708	-3.597	3.111
Inh 6-1p	-9.088	-7.717	1.371	Inh 6-1pw	-6.861	-3.579	3.283
Inh 1-1p	-9.076	-6.603	2.473	Inh 1-1pw	-6.787	-2.343	4.444
Inh 2-1p	-8.577	-6.436	2.140	Inh 2-1pw	-6.428	-2.283	4.145
Inh 3-1p	-9.481	-6.699	2.782	Inh 3-1pw	-7.025	-2.547	4.478
Inh 4-1p	-8.722	-6.509	2.213	Inh 4-1pw	-6.463	-2.379	4.083
Inh 5-1p	-9.156	-6.620	2.536	Inh 5-1pw	-6.828	-2.486	4.342
Inh 6-1p	-9.070	-6.728	2.342	Inh 6-1pw	-6.932	-2.649	4.284

p: protonated, pw: water phase with protonated

Table S4. The calculated other quantum chemical parameters for the protonated for gas and solvent phase compounds by using B3LYP/6-311++G(2d,2p), B3LYP/cc-pVTZ and BP86/6-311++G(2d,2p) methods.

Mol.	η, eV	σ, eV^{-1}	χ, eV	ω, eV	ε, eV^{-1}	D, Debye	Energy, eV
B3LYP/6-311++G(2d,2p)							
Inh 1-1p	1.841	0.543	7.906	16.976	0.059	4.420	-25897.015
Inh 2-1p	1.669	0.599	7.591	17.259	0.058	4.042	-27944.119
Inh 3-1p	1.923	0.520	8.198	17.470	0.057	4.301	-23757.827
Inh 4-1p	1.703	0.587	7.652	17.197	0.058	4.413	-26874.622
Inh 5-1p	1.834	0.545	7.946	17.210	0.058	6.263	-25896.860
Inh 6-1p	1.730	0.578	8.060	18.776	0.053	11.734	-93788.209
Inh 1-1p	2.220	0.450	7.998	14.409	0.069	2.215	-25901.927
Inh 2-1p	2.016	0.496	7.636	14.459	0.069	2.436	-27943.984
Inh 3-1p	2.238	0.447	8.566	16.392	0.061	0.495	-23757.567
Inh 4-1p	1.982	0.505	7.875	15.650	0.064	2.013	-26874.399

Inh 5-1p	2.157	0.464	8.160	15.432	0.065	3.945	-25896.693
Inh 6-1p	1.929	0.518	8.322	17.955	0.056	8.930	-93787.940
Inh 1-1p	1.422	0.703	8.120	23.185	0.043	4.788	-25897.480
Inh 2-1p	1.398	0.715	7.937	22.535	0.044	5.925	-27944.648
Inh 3-1p	1.332	0.751	8.494	27.087	0.037	5.201	-23757.771
Inh 4-1p	1.220	0.819	8.081	26.758	0.037	6.537	-26875.006
Inh 5-1p	1.187	0.842	8.287	28.922	0.035	4.361	-25897.159
Inh 6-1p	1.309	0.764	8.494	27.565	0.036	3.228	-93788.145
Inh 1-1p	1.923	0.520	7.753	15.627	0.064	7.382	-25897.756
Inh 2-1p	1.732	0.577	7.435	15.962	0.063	7.413	-27944.876
Inh 3-1p	2.088	0.479	8.016	15.388	0.065	6.778	-23758.589
Inh 4-1p	1.767	0.566	7.537	16.077	0.062	7.473	-26875.393
Inh 5-1p	1.956	0.511	7.800	15.553	0.064	8.719	-25897.623
Inh 6-1p	1.846	0.542	7.850	16.687	0.060	15.529	-93788.971
B3LYP/cc-pVTZ							
Inh 1-1p	1.853	0.540	7.874	16.730	0.060	4.429	-25897.955
Inh 2-1p	1.679	0.595	7.548	16.964	0.059	4.013	-27945.161
Inh 3-1p	1.933	0.517	8.165	17.244	0.058	4.299	-23758.674
Inh 4-1p	1.711	0.585	7.610	16.924	0.059	4.379	-26875.622
Inh 5-1p	1.845	0.542	7.916	16.985	0.059	6.277	-25897.802
Inh 6-1p	1.739	0.575	8.028	18.526	0.054	11.671	-93791.430
Inh 1-1p	2.237	0.447	7.960	14.166	0.071	2.206	-25897.761
Inh 2-1p	2.034	0.492	7.582	14.130	0.071	2.323	-27945.006
Inh 3-1p	2.246	0.445	8.513	16.134	0.062	0.417	-23758.393
Inh 4-1p	2.024	0.494	7.754	14.854	0.067	2.356	-26875.459
Inh 5-1p	2.175	0.460	8.121	15.162	0.066	3.956	-25897.613
Inh 6-1p	1.948	0.513	8.284	17.608	0.057	8.841	-93791.138
Inh 1-1p	1.433	0.698	8.071	22.737	0.044	4.656	-25898.415
Inh 2-1p	1.400	0.714	7.878	22.168	0.045	5.860	-27945.684
Inh 3-1p	1.329	0.753	8.429	26.734	0.037	5.231	-23758.668
Inh 4-1p	1.204	0.831	8.014	26.677	0.037	6.620	-26875.999
Inh 5-1p	1.179	0.848	8.233	28.749	0.035	4.337	-25898.092
Inh 6-1p	1.305	0.766	8.430	27.233	0.037	3.246	-93791.419
Inh 1-1p	1.961	0.510	7.676	15.022	0.067	7.546	-25898.707
Inh 2-1p	1.762	0.568	7.350	15.330	0.065	7.537	-27945.935
Inh 3-1p	2.117	0.472	7.952	14.935	0.067	6.849	-23759.455
Inh 4-1p	1.794	0.557	7.453	15.476	0.065	7.601	-26876.410
Inh 5-1p	1.445	0.692	8.276	23.694	0.042	8.837	-25898.583
Inh 6-1p	1.874	0.534	7.787	16.184	0.062	15.582	-93792.208
BP86/6-311++G(2d,2p)							
Inh 1-1p	1.186	0.843	7.960	26.709	0.037	3.931	-25897.922
Inh 2-1p	1.038	0.963	7.629	28.028	0.036	3.263	-27945.176
Inh 3-1p	1.260	0.793	8.268	27.119	0.037	3.996	-23758.793
Inh 4-1p	1.072	0.933	7.701	27.663	0.036	3.698	-26875.705
Inh 5-1p	1.187	0.842	8.010	27.015	0.037	5.739	-25897.731
Inh 6-1p	1.084	0.922	8.104	30.286	0.033	10.997	-93796.111
Inh 1-1p	1.485	0.674	8.069	21.930	0.046	1.847	-25897.710
Inh 2-1p	1.308	0.765	7.695	22.640	0.044	1.946	-27944.994
Inh 3-1p	1.435	0.697	8.526	25.338	0.039	0.408	-23758.493
Inh 4-1p	1.306	0.766	7.857	23.633	0.042	1.896	-26875.520

Inh 5-1p	1.433	0.698	8.212	23.526	0.043	3.560	-25897.528
Inh 6-1p	1.248	0.802	8.349	27.941	0.036	8.533	-93795.797
Inh 1-1p	0.764	1.309	8.063	42.545	0.024	4.026	-25898.274
Inh 2-1p	0.742	1.347	7.861	41.627	0.024	5.280	-27945.595
Inh 3-1p	0.696	1.437	8.444	51.214	0.020	4.397	-23758.722
Inh 4-1p	0.552	1.811	8.002	57.972	0.017	5.928	-26875.993
Inh 5-1p	0.585	1.708	8.225	57.770	0.017	3.355	-25897.952
Inh 6-1p	0.685	1.459	8.402	51.507	0.019	3.814	-93796.031
Inh 1-1p	1.237	0.809	7.839	24.849	0.040	6.770	-25898.542
Inh 2-1p	1.070	0.934	7.506	26.324	0.038	6.530	-27945.822
Inh 3-1p	1.391	0.719	8.090	23.528	0.043	6.514	-23759.439
Inh 4-1p	1.106	0.904	7.615	26.206	0.038	6.551	-26876.362
Inh 5-1p	1.268	0.789	7.888	24.531	0.041	8.156	-25898.378
Inh 6-1p	1.171	0.854	7.899	26.643	0.038	14.892	-93796.747
B3LYP/6-311++G(2d,2p)							
Inh 1-1pw	1.971	0.507	4.735	5.688	0.176	6.044	-25899.285
Inh 2-1pw	1.845	0.542	4.557	5.630	0.178	5.756	-27946.379
Inh 3-1pw	2.000	0.500	4.879	5.950	0.168	5.848	-23760.215
Inh 4-1pw	1.843	0.543	4.581	5.692	0.176	6.265	-26876.935
Inh 5-1pw	1.947	0.514	4.770	5.843	0.171	8.155	-25888.488
Inh 6-1pw	1.939	0.516	4.891	6.169	0.162	14.453	-93790.665
Inh 1-1pw	2.410	0.415	4.816	4.812	0.208	2.693	-25904.076
Inh 2-1pw	2.222	0.450	4.545	4.647	0.215	4.151	-27946.064
Inh 3-1pw	2.304	0.434	5.074	5.586	0.179	1.005	-23759.813
Inh 4-1pw	2.153	0.464	4.693	5.115	0.196	3.370	-26876.561
Inh 5-1pw	2.296	0.436	4.930	5.293	0.189	4.843	-25898.870
Inh 6-1pw	2.230	0.449	5.115	5.868	0.170	10.914	-93790.255
Inh 1-1pw	1.699	0.589	5.002	7.365	0.136	8.136	-25899.748
Inh 2-1pw	1.738	0.576	4.937	7.013	0.143	8.665	-27946.900
Inh 3-1pw	1.677	0.596	5.170	7.967	0.126	7.710	-23760.265
Inh 4-1pw	1.636	0.611	5.036	7.748	0.129	9.345	-26877.327
Inh 5-1pw	1.556	0.643	5.152	8.533	0.117	7.312	-25899.476
Inh 6-1pw	1.641	0.609	5.220	8.300	0.120	3.033	-93790.663
Inh 1-1pw	2.222	0.450	4.565	4.690	0.213	10.859	-25899.761
Inh 2-1pw	2.072	0.483	4.355	4.577	0.218	11.521	-27946.867
Inh 3-1pw	2.239	0.447	4.786	5.115	0.196	9.655	-23760.732
Inh 4-1pw	2.042	0.490	4.421	4.787	0.209	11.636	-26877.401
Inh 5-1pw	2.171	0.461	4.657	4.994	0.200	12.085	-25899.664
Inh 6-1pw	2.142	0.467	4.790	5.357	0.187	19.866	-93791.206
B3LYP/cc-pVTZ							
Inh 1-1pw	1.985	0.504	4.688	5.536	0.181	6.052	-25900.219
Inh 2-1pw	1.855	0.539	4.501	5.542	0.180	5.725	-27947.414
Inh 3-1pw	2.013	0.497	4.833	5.800	0.172	5.843	-23761.057
Inh 4-1pw	1.853	0.540	4.527	5.530	0.181	6.195	-26877.907
Inh 5-1pw	1.960	0.510	4.727	5.698	0.175	8.192	-25900.100
Inh 6-1pw	1.949	0.513	4.846	6.023	0.166	14.393	-93793.882
Inh 1-1pw	2.429	0.412	4.768	4.680	0.214	2.648	-25899.856
Inh 2-1pw	2.234	0.448	4.478	4.487	0.223	3.707	-27947.088
Inh 3-1pw	2.315	0.432	5.015	5.432	0.184	0.893	-23760.640
Inh 4-1pw	2.182	0.458	4.600	4.848	0.206	3.698	-26877.609

Inh 5-1pw	2.311	0.433	4.880	5.152	0.194	4.896	-25899.779
Inh 6-1pw	2.246	0.445	5.068	5.718	0.175	10.788	-93793.452
Inh 1-1pw	1.687	0.593	4.938	7.228	0.138	7.992	-25900.703
Inh 2-1pw	1.726	0.579	4.866	6.859	0.146	8.605	-27947.929
Inh 3-1pw	1.675	0.597	5.097	7.755	0.129	7.647	-23761.115
Inh 4-1pw	1.622	0.616	4.962	7.590	0.132	9.364	-26878.318
Inh 5-1pw	1.538	0.650	5.087	8.416	0.119	7.225	-25900.415
Inh 6-1pw	0.928	1.078	5.158	14.331	0.070	3.768	-93798.443
Inh 1-1pw	2.240	0.446	4.511	4.542	0.220	10.917	-25900.713
Inh 2-1pw	2.100	0.476	4.273	4.346	0.230	11.510	-27947.914
Inh 3-1pw	2.268	0.441	4.717	4.906	0.204	9.710	-23761.579
Inh 4-1pw	2.067	0.484	4.341	4.558	0.219	11.632	-26878.409
Inh 5-1pw	2.202	0.454	4.588	4.781	0.209	12.183	-25900.613
Inh 6-1pw	2.168	0.461	4.725	5.150	0.194	19.867	-93794.435
BP86/6-311++G(2d,2p)							
Inh 1-1pw	1.278	0.782	4.803	9.023	0.111	5.798	-25900.122
Inh 2-1pw	1.159	0.863	4.611	9.175	0.109	5.143	-27947.368
Inh 3-1pw	1.312	0.762	4.957	9.368	0.107	5.728	-23761.131
Inh 4-1pw	1.693	0.591	4.121	5.015	0.199	5.625	-26877.926
Inh 5-1pw	1.268	0.788	4.850	9.274	0.108	7.915	-25899.973
Inh 6-1pw	1.251	0.800	4.956	9.818	0.102	14.174	-93798.487
Inh 1-1pw	1.627	0.614	4.881	7.318	0.137	2.559	-25899.740
Inh 2-1pw	1.474	0.678	4.618	7.233	0.138	3.761	-27947.002
Inh 3-1pw	1.473	0.679	5.070	8.726	0.115	0.951	-23760.690
Inh 4-1pw	1.426	0.701	4.732	7.853	0.127	3.256	-26877.611
Inh 5-1pw	1.508	0.663	4.979	8.222	0.122	4.476	-25899.629
Inh 6-1pw	1.431	0.699	5.121	9.163	0.109	10.684	-93798.042
Inh 1-1pw	0.938	1.066	4.967	13.157	0.076	7.541	-25900.481
Inh 2-1pw	0.978	1.023	4.887	12.213	0.082	8.581	-27947.778
Inh 3-1pw	0.951	1.051	5.125	13.801	0.072	6.785	-23761.127
Inh 4-1pw	0.875	1.142	4.985	14.192	0.070	9.398	-26878.236
Inh 5-1pw	0.785	1.274	5.112	16.646	0.060	7.027	-25900.204
Inh 6-1pw	0.928	1.078	5.158	14.331	0.070	3.768	-93798.443
Inh 1-1pw	1.471	0.680	4.659	7.377	0.136	10.623	-25900.520
Inh 2-1pw	1.326	0.754	4.442	7.440	0.134	10.894	-27947.763
Inh 3-1pw	1.502	0.666	4.855	7.850	0.127	9.666	-23761.489
Inh 4-1pw	1.319	0.758	4.499	7.674	0.130	11.043	-26878.339
Inh 5-1pw	1.448	0.691	4.737	7.752	0.129	11.920	-25900.375
Inh 6-1pw	1.412	0.708	4.848	8.323	0.120	19.691	-93798.907

p: protonated, pw: water phase with protonated

Table S5. Calculated Mulliken charges on sulfur atom in studied molecules.

Molecule	B3LYP/6-311++G(2d,2p)	B3LYP/cc-pVTZ	BP86/6-311++G(2d,2p)
Inh 1	-0.583475	-0.394873	-0.602524
Inh 2	-0.515301	-0.399189	-0.615810
Inh 3	-0.528485	-0.385720	-0.605219
Inh 4	-0.541685	-0.396314	-0.622850

Inh 5	-0.529346	-0.390308	-0.606624
Inh 6	-0.522600	-0.378696	-0.602654